Supporting Information

>1000-Fold Lifetime Extension of Nickel Electromechanical Contact Device via Graphene

Min-Ho Seo[†], *Jae-Hyeon Ko*[‡], *Jeong Oen Lee*[†, §], *Seung-Deok Ko*[†, ∥], *Jeong Hun Mun*[†], *Byung Jin Cho*[†], *Yong-Hyun Kim*[‡]*, *and Jun-Bo Yoon*[†]*

[†] School of Electrical Engineering, Korea Advanced Institute of Science and Technology (KAIST), 291 Daehak-ro, Yuseong-gu, Daejeon 34141, Republic of Korea

[‡] Graduate School of Nanoscience and Technology, Korea Advanced Institute of Science and Technology (KAIST), 291 Daehak-ro, Yuseong-gu, Daejeon 34141, Republic of Korea

[§] Present address: Department of Electrical Engineering, California Institute of Technology, Pasadena, CA 91125, USA.

[∥] Present address: Department of Electrical and Computer Engineering, Georgia Institute of Technology, Atlanta, GA 30308, USA.

*Correspondence to: jbyoon@kaist.ac.kr (Tel: +82-42-350-3476, Fax: +82-42-350-8565) and yong.hyun.kim@kaist.ac.kr (Tel: +82-42-350-1111, Fax: +82-42-350-1110)

Keywords: Graphene, MEMS/NEMS, mechanical switch, lubrication, reliability

Contents

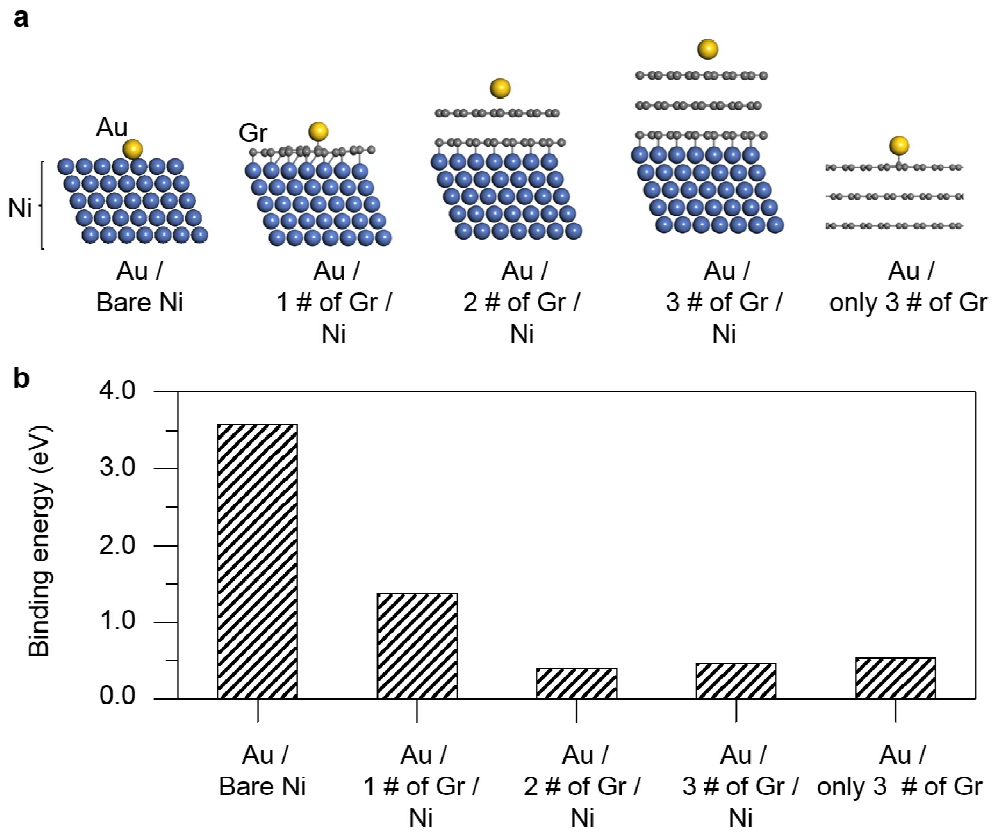

Figure S1. Binding energy calculations of gold (Au) and nickel (Ni) surfaces coated with layers of graphene (Gr). (a) Designs of atomic structures and (b) calculated binding energies. A single layer of Gr coating Ni remarkably lowered the binding energy with Au by ~62%. The binding energy of Au and three-layer Gr is the same with or without the underlying Ni.

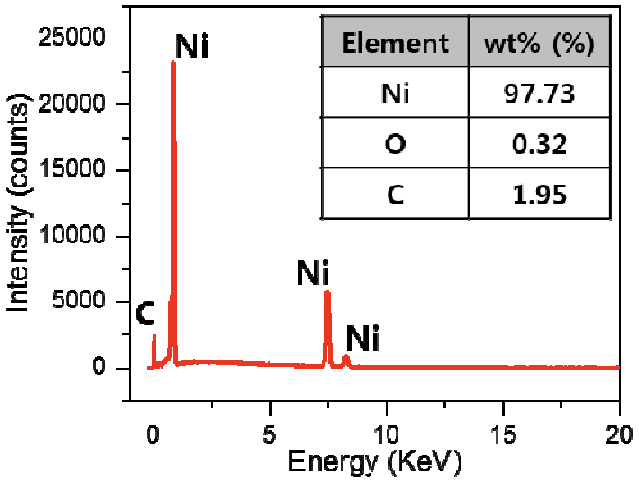

Figure S2. EDS (energy dispersive X-ray spectroscope) analysis result of the surface cleaned nickel.

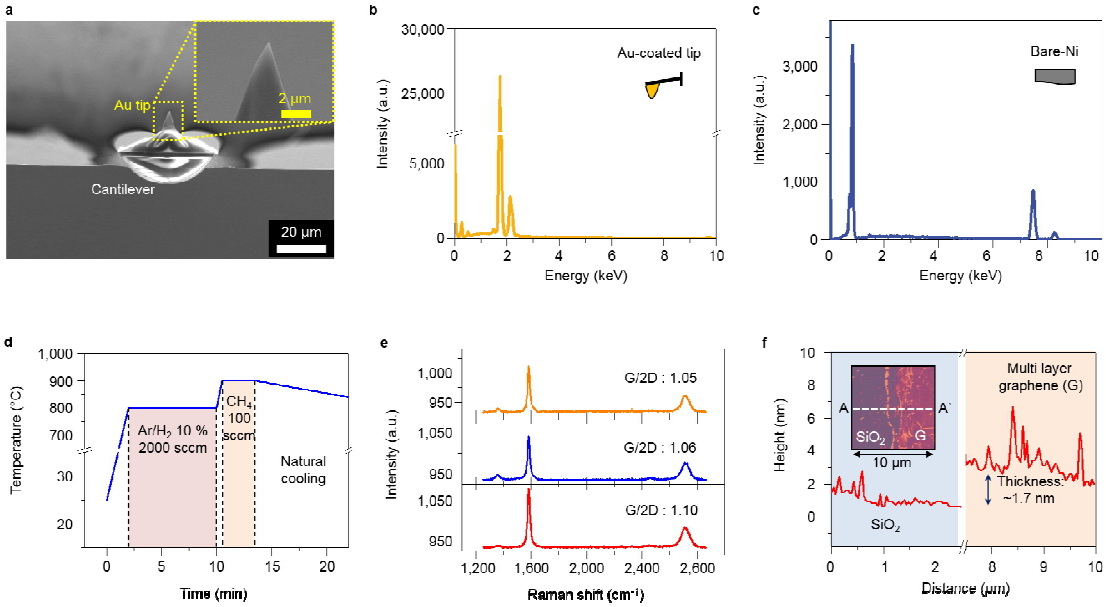

Figure S3. Atomic force microscopy (AFM) force–distance experimental details. (a) Scanning electron microscopy image of the gold (Au)-coated AFM tip. Energy dispersive spectroscopy data for the (b) Au-coated tip and (c) electroplated nickel (Ni) sample. (d) Conditions for chemical vapour deposition of graphene. (e) Raman spectrum of synthesized graphene. High-quality multilayer graphene formation was confirmed at three different points. (f) Thickness of the synthesized graphene layer measured by AFM after transfer onto Ni by etching of a flat silicon dioxide wafer.

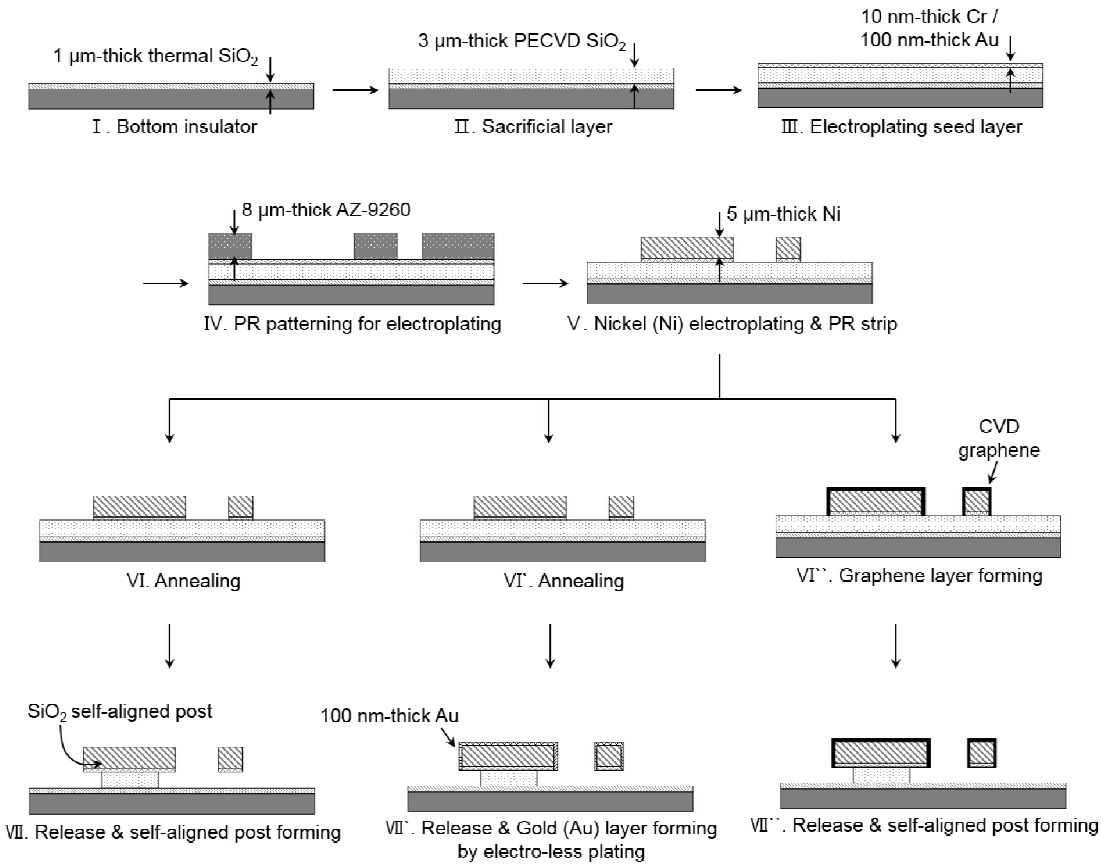

Figure S4. Schematic illustrations of nickel (Ni), gold (Au), and graphene (Gr) contacting devices. The experimental conditions are specifically contained in the Experimental section in manuscript.

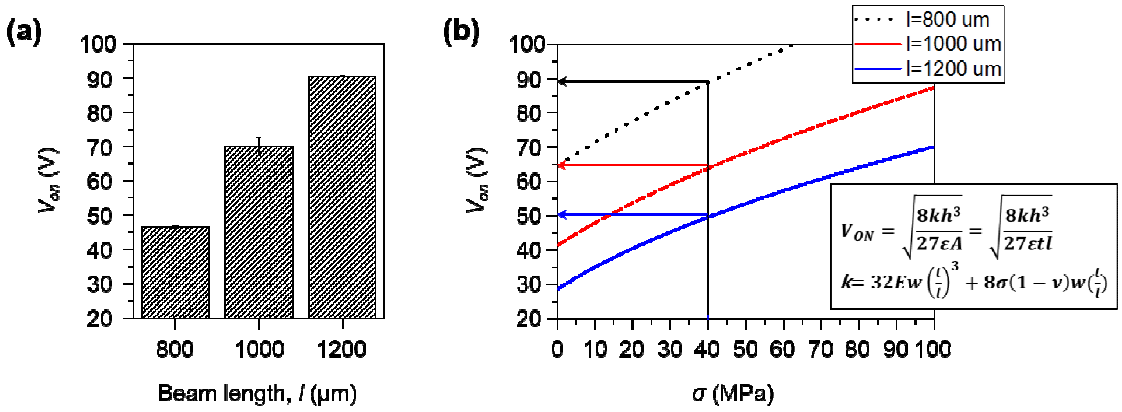

Figure S5. (a) Measured on-voltage (V_{on}) of devices, having different beam length (l). (b) Theoretical calculation of V_{on} of devices considering residual stress (σ). Solid allow lines indicate the V_{on} of devices with σ=40 MPa.

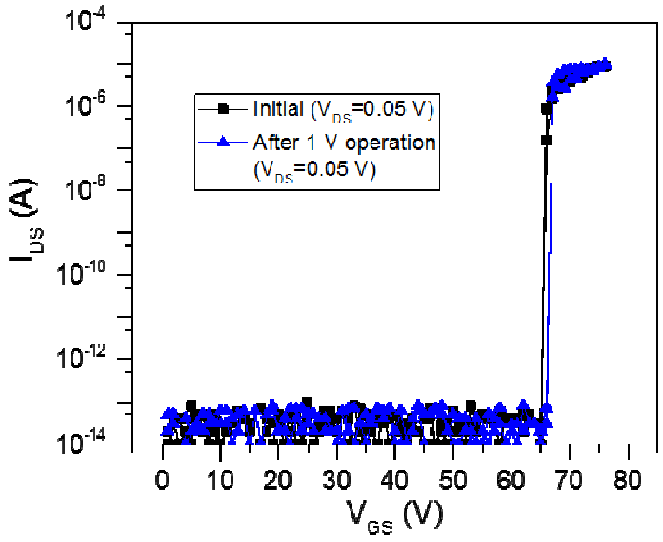

Figure S6. I-V curve comparison of graphene contact device before and after VDS=1 V operation. I-V curve was measured with VDS=0.05 V.

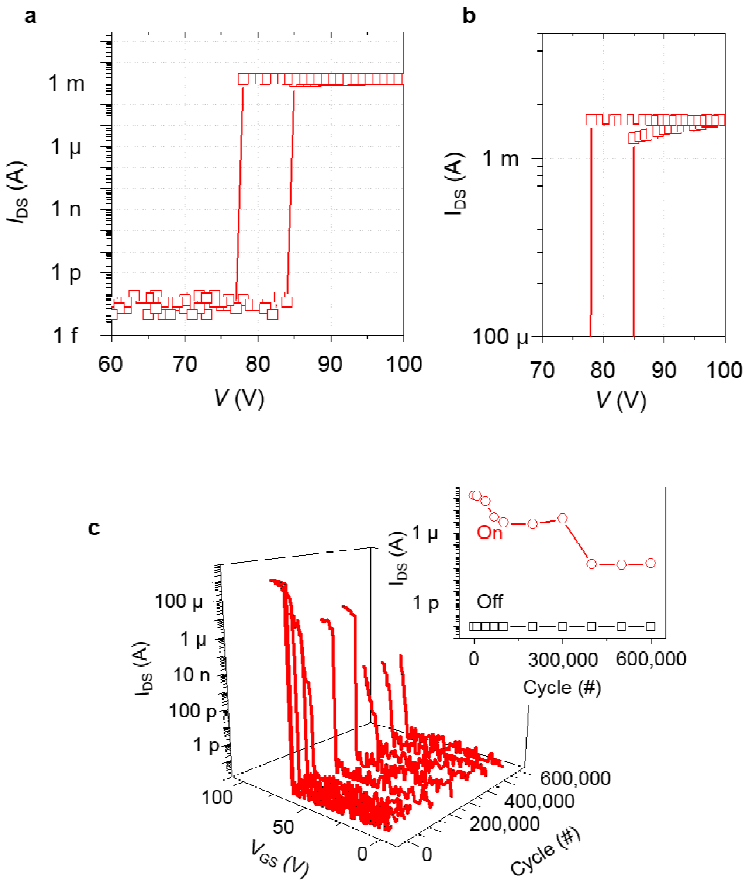

Figure S7. Current–voltage (I-V) characteristics of a gold (Au)-contacting microelectromechanical switch. (a) Measured I-V curve without current compliance. (b) Magnified I-V characteristics in the mechanically contacted range. Strong adhesive properties similar to those of the nickel (Ni)-contacting device are confirmed. (c) Long-term reliability characteristics under 1 μA/1 V hot-switching conditions. Marked performance degradation after 300,000 cycles is observed.